

# Computing Bisimulation Functions using SOS Optimization and $\delta$ -Decidability over the Reals

Abhishek Murthy  
 Stony Brook University  
 Stony Brook, NY, USA  
 amurthy@cs.sunysb.edu

Scott A. Smolka  
 Stony Brook University  
 Stony Brook, NY, USA  
 sas@cs.sunysb.edu

Md. Ariful Islam  
 Stony Brook University  
 Stony Brook, NY, USA  
 mdaislam@cs.sunysb.edu

Radu Grosu  
 Vienna Univ. of Technology  
 Vienna, Austria  
 radu.grosu@tuwien.ac.at

## ABSTRACT

We present *BFComp*, an automated framework based on Sum-Of-Squares (SOS) optimization and  $\delta$ -decidability over the reals, to compute Bisimulation Functions (BFs) that characterize Input-to-Output Stability (IOS) of dynamical systems. BFs are Lyapunov-like functions that decay along the trajectories of a given pair of systems, and can be used to establish the stability of the outputs with respect to bounded input deviations.

In addition to establishing IOS, *BFComp* is designed to provide tight bounds on the squared output errors between systems whenever possible. For this purpose, two SOS optimization formulations are employed: SOSP 1, which enforces the decay requirements on a discretized grid over the input space, and SOSP 2, which covers the input space exhaustively. SOSP 2 is attempted first, and if the resulting error bounds are not satisfactory, SOSP 1 is used to compute a *Candidate BF* (CBF). The decay requirement for the BFs is then encoded as a  $\delta$ -decidable formula and validated over a level set of the CBF using the dReal tool. If dReal produces a counterexample containing the states and inputs where the decay requirement is violated, this pair of vectors is used to refine the input-space grid and SOSP 1 is iterated.

By computing BFs that appeal to a small-gain theorem, the *BFComp* framework can be used to show that a subsystem of a feedback-composed system can be replaced—with bounded error—by an approximately equivalent abstraction, thereby enabling approximate model-order reduction of dynamical systems. We illustrate the utility of *BFComp* on a canonical cardiac-cell model, showing that the four-variable Markovian model for the slowly activating Potassium current  $I_{K_s}$  can be safely replaced by a one-variable Hodgkin-Huxley-type approximation.

Permission to make digital or hard copies of part or all of this work for personal or classroom use is granted without fee provided that copies are not made or distributed for profit or commercial advantage and that copies bear this notice and the full citation on the first page. Copyrights for third-party components of this work must be honored. For all other uses, contact the Owner/Author.

Copyright is held by the owner/author(s).

HSCC '15, Apr 14-16, 2015, Seattle, WA, USA

Copyright 2015 ACM ACM 978-1-4503-3433-4/15/04

<http://dx.doi.org/10.1145/2728606.2728609>.

## 1. INTRODUCTION

Incremental *Input-to-State Stability* (ISS) of a pair of dynamical systems refers to the property that bounded differences in their input signals lead to bounded differences in their resulting state trajectories. Incremental *Input-to-Output Stability* (IOS) generalizes incremental ISS to systems with output maps. Since the seminal work of Sontag [29, 30, 31], the  $\mathcal{K}$ ,  $\mathcal{KL}$ , and  $\mathcal{K}_\infty$  classes of Kamke functions have been used to characterize ISS of dynamical systems as extensions of Lyapunov stability; see [18]. These Lyapunov-like functions have been used in the small-gain theorems of [34] to establish stability of feedback-based interconnected systems, thereby enabling compositional design of nonlinear control systems.

Similar to Kamke and Lyapunov functions, *Bisimulation Functions* (BFs) have played a transformative role in extending the control-theoretic notions of Lyapunov Stability and ISS to system verification. BFs [8, 9, 10, 1, 15] are Lyapunov-like functions that decay along the trajectories of a given pair of dynamical systems. Level sets of BFs yield approximate bisimulation relations that generalize the classical notion of bisimulation equivalence of finite-state systems [23] to real-valued continuous-time dynamical systems. BFs also allow one to show that a system is robust to bounded deviations in the input signals.

BFs can also be used to reason *compositionally* about dynamical systems. Consider a dynamical system  $D$  with a subsystem  $S$  connected to the rest of  $D$  through a feedback loop. Moreover, suppose we have an approximately equivalent version  $S'$  of  $S$  that uses fewer state variables than  $S$ . That is,  $S'$  is an *abstraction* or model-order reduction of  $S$ , and by substituting  $S'$  for  $S$  in  $D$  one would hope to obtain the corresponding model-order reduction in  $D$ . Care must be taken in this situation, however, as the approximation error between  $S$  and  $S'$  may get amplified by the feedback context in which  $S$  resides.

As shown in [1, 21], one can appeal to a small-gain theorem to compute BFs that *bound the error* that is introduced when substituting  $S'$  for  $S$  within  $D$ . BFs can also be used in other system design and verification settings, including controller design [11], reachability analysis [19], and simulation-based verification [12, 4].

In this paper, we present *BFComp*: an automated framework for computing BFs that characterize IOS of dynamical

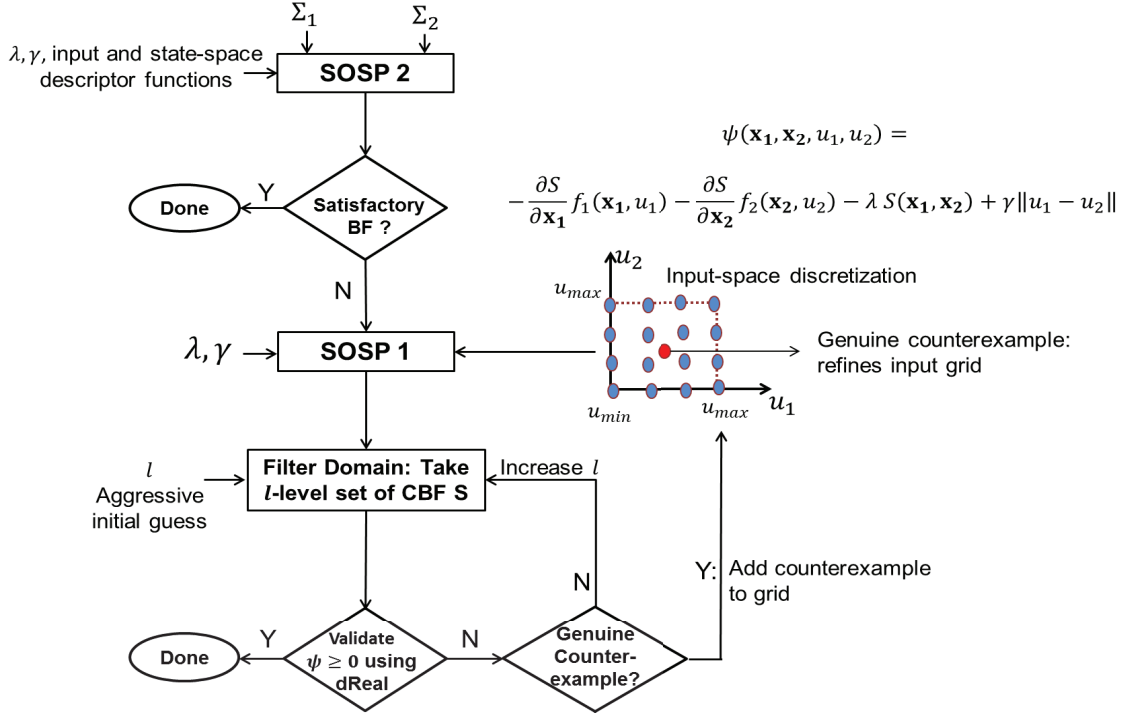


Figure 1: *BFCOMP*: An Automated Framework for Computing BFs using SOS Optimization and  $\delta$ -decidability.

systems. *BFCOMP*, which is illustrated in Fig. 1, leverages Sum-Of-Squares (SOS) optimization and  $\delta$ -decidability over the reals [7], a new form of Satisfiability Modulo Theory (SMT), to compute BFs. In addition to establishing IOS, *BFCOMP* is designed to provide tight bounds on the squared output errors between systems whenever possible.

An overview of *BFCOMP* is as follows. Given a pair of dynamical systems  $\Sigma_1$  and  $\Sigma_2$ , an SOS Problem (SOSP) called SOSP 2 is formulated and solved using MATLAB SOSTOOLS [26]. SOSP 2 requires the decay parameter  $\lambda$ , the gain parameter  $\gamma$ , and so-called *descriptor functions* that characterize the bounded state and input spaces. If the resulting BF provides satisfactory bounds on the output error, then the BF computation terminates.

Otherwise, an alternative SOSP formulation, SOSP 1, is called upon. SOSP 1, which we recently proposed in [21], uses  $\lambda$  and  $\gamma$  to compute a *Candidate BF* (CBF) that satisfies the decay condition of [1] only across a discretized grid over the bounded input space. *BFCOMP* then appeals to the  $\delta$ -decidability-based dReal [7] to verify that the decay requirement, which is encoded by the SMT formula  $\psi$ , is exhaustively satisfied over the exterior of the CBF’s  $l$ -level set.

Level sets are used here because dReal relies fundamentally on the technique of  $\delta$ -relaxation, which may lead to spurious counterexamples. Taking the level set of the CBF filters out the origin and a finite-sized neighborhood around it, which gives rise to the spurious counterexamples. Starting from a relatively small (aggressive) value, which retains most of the state space in the domain of  $\psi$ , the parameter  $l$  is (iteratively) tuned to filter  $\psi$ ’s domain to avoid such counterexamples. A positive result by dReal implies that the CBF is actually a valid BF everywhere outside the  $l$ -

level set. If a (genuine) counterexample  $\mathbf{c} = (\mathbf{x}_1, \mathbf{x}_2, u_1, u_2)$  to  $\psi$  is found, then  $\mathbf{c}$  is used to refine the input-space grid.

To illustrate the utility of *BFCOMP*, we apply it to the model-order reduction of a canonical cardiac-cell model [21]. In particular, we use our framework to compute BFs that appeal to the small-gain theorem of [1] to establish that the four-variable Markovian potassium-channel component of the cell model can be safely replaced by an approximately equivalent one-variable abstraction. The canonical model captures the feedback-based interconnection of the four-variable model within the detailed 67-variable Iyer-Mazhari-Winslow (IMW) ventricular cell model [32]. To the best of our knowledge, this is the first compositional proof of a feedback-based approximate model-order reduction of a biological system.

The rest of the paper develops along the follow lines. Section 2 reviews basic definitions and properties of BFs from [1], our previous work on SOSP 1 [21], and the four-variable potassium channel model from [32]. Section 2.4 discusses the one-variable potassium channel abstraction. Section 3 describes our BF-based approach to establishing the substitutivity result within the canonical cell model. Section 4 presents SOSP 2, while Section 5 considers our dReal-based validation of SOSP 1 CBFs. Section 6 presents the results of our case study and highlights the implementation issues we faced with *BFCOMP*. Section 7 considers related work. Section 8 contains our concluding remarks and directions for future work.

## 2. BACKGROUND

In this section, we review the results on BFs from [1] and our input-space sampling-based algorithm from [21].

Then, we present physiological background by introducing the four-variable Markovian subsystem for the  $I_{K_s}$  current of the IMW model.

We define dynamical systems using a 6-tuple  $(\mathcal{X}, \mathcal{X}^0, \mathcal{U}, f, \mathcal{O}, g)$ , where  $\mathcal{X}$  is the *state space*,  $\mathcal{X}^0 \subseteq \mathcal{X}$  is the set of *initial conditions*,  $\mathcal{U}$  is the *input space*,  $f: \mathcal{X} \times \mathcal{U} \rightarrow \mathcal{X}$  is the *vector field* defining the dynamics,  $\mathcal{O}$  is the set of *outputs*, and  $g: \mathcal{X} \rightarrow \mathcal{O}$  maps a state to its output.

## 2.1 Bisimulation Functions

BFs [1] are non-increasing functions that characterize the joint IOS of two dynamical systems. The following definition, adapted from [1], uses  $\| \cdot \|$  to denote the squared L2-norm.

*Definition 1.* Let  $\Sigma_i = (\mathcal{X}_i, \mathcal{X}_i^0, \mathcal{U}, f_i, \mathcal{Y}, g_i)$ ,  $i = 1, 2$ , be two dynamical systems such that  $\mathcal{X}_i \subseteq \mathbb{R}^{n_i}$ ,  $\mathcal{U} \subseteq \mathbb{R}^m$  and  $\mathcal{Y} \subseteq \mathbb{R}^p$ . A *bisimulation function* (BF) is a smooth function  $S: \mathbb{R}^{n_1} \times \mathbb{R}^{n_2} \rightarrow \mathbb{R}_{\geq 0}$  such that for every  $\mathbf{x}_1 \in \mathcal{X}_1$ ,  $\mathbf{x}_2 \in \mathcal{X}_2$ ,  $\mathbf{u}_1, \mathbf{u}_2 \in \mathcal{U}$ :

$$\|g_1(\mathbf{x}_1) - g_2(\mathbf{x}_2)\| \leq S(\mathbf{x}_1, \mathbf{x}_2), \quad (1)$$

$\exists \lambda > 0, \gamma \geq 0$  such that  $\forall \mathbf{x}_1, \mathbf{x}_2, \mathbf{u}_1, \mathbf{u}_2$ :

$$\frac{\partial S}{\partial \mathbf{x}_1} f_1(\mathbf{x}_1, \mathbf{u}_1) + \frac{\partial S}{\partial \mathbf{x}_2} f_2(\mathbf{x}_2, \mathbf{u}_2) \leq -\lambda S(\mathbf{x}_1, \mathbf{x}_2) + \gamma \|\mathbf{u}_1 - \mathbf{u}_2\|. \quad (2)$$

■

Next, we present a modified version of Theorem 1 of [1], which captures the joint IOS of two systems.

*Theorem 1.* Let  $S$  be a BF with parameters  $\lambda$  and  $\gamma$  between dynamical systems  $\Sigma_i$ ,  $i = 1, 2$ , and let  $\mathbf{x}_1(t)$  and  $\mathbf{x}_2(t)$  be two trajectories of the systems. For all  $t \geq 0$ ,

$$\begin{aligned} \|g_1(\mathbf{x}_1(t)) - g_2(\mathbf{x}_2(t))\| &\leq S(\mathbf{x}_1(t), \mathbf{x}_2(t)) \\ &\leq e^{-\lambda t} S(\mathbf{x}_1(0), \mathbf{x}_2(0)) + \\ &\quad \frac{\gamma}{\lambda} \|\mathbf{u}_1 - \mathbf{u}_2\|_{\infty}, \end{aligned}$$

where  $\|\mathbf{u}_1 - \mathbf{u}_2\|_{\infty} = \sup_{t \geq 0} \|\mathbf{u}_1(t) - \mathbf{u}_2(t)\|$  is the maximum difference in the input signals of the two systems.

PROOF. See the supplementary document [20]. □

The *feedback composition*  $\Sigma_A || \Sigma_B$  of two dynamical systems  $\Sigma_A$  and  $\Sigma_B$  is obtained by feeding the output of  $\Sigma_A$  as the input to  $\Sigma_B$  and vice versa. When subsystems are connected using feedback, their respective BF's can be composed subject to a small-gain condition. We formalize this idea by stating a result based on Theorem 2 of [1].

*Theorem 2.* Let  $\Sigma_i = (\mathcal{X}_i, \mathcal{X}_i^0, \mathcal{U}_i, f_i, \mathcal{O}_i, g_i)$ ,  $i = 1, 2, A, B$ , be dynamical systems such that  $\mathcal{U}_1 = \mathcal{O}_A$ ,  $\mathcal{U}_A = \mathcal{O}_1$ ,  $\mathcal{U}_2 = \mathcal{O}_B$  and  $\mathcal{U}_B = \mathcal{O}_2$ . Let  $S_{12}$ , parameterized by  $\lambda_{12}$  and  $\gamma_{12}$ , be a BF between  $\Sigma_1$  and  $\Sigma_2$ . Let  $S_{AB}$ , parameterized by  $\lambda_{AB}$  and  $\gamma_{AB}$ , be a BF between  $\Sigma_A$  and  $\Sigma_B$ .

Let  $\Sigma_{A1} = \Sigma_A || \Sigma_1$  and  $\Sigma_{B2} = \Sigma_B || \Sigma_2$ . If the *Small-Gain Condition* (SGC)  $\frac{\gamma_{AB}\gamma_{12}}{\lambda_{AB}\lambda_{12}} < 1$  is met, then a BF  $S$  can be constructed between  $\Sigma_{A1}$  and  $\Sigma_{B2}$  by composing  $S_{AB}$  and  $S_{12}$  as follows:

$$S(\mathbf{x}_{A1}, \mathbf{x}_{B2}) = \alpha_1 S_{AB}(\mathbf{x}_A, \mathbf{x}_B) + \alpha_2 S_{12}(\mathbf{x}_1, \mathbf{x}_2) \quad (3)$$

where  $\mathbf{x}_{A1} = [\mathbf{x}_A, \mathbf{x}_1]^T$  and  $\mathbf{x}_{B2} = [\mathbf{x}_B, \mathbf{x}_2]^T$  and the constants  $\alpha_1$  and  $\alpha_2$  are given by:

$$\begin{cases} \frac{\gamma_{12}}{\lambda_{AB}} < \alpha_1 < \frac{\lambda_{12}}{\gamma_{AB}} & \text{and } \alpha_2 = 1 & \text{if } \lambda_{AB} \leq \gamma_{12} \\ \alpha_1 = 1 & \text{and } \frac{\gamma_{AB}}{\lambda_{12}} < \alpha_2 < \frac{\lambda_{AB}}{\gamma_{12}} & \text{if } \lambda_{12} \leq \gamma_{AB} \\ \alpha_1 = 1 & \text{and } \alpha_2 = 1 & \text{in other cases} \end{cases} \quad (4)$$

PROOF. See the supplementary document [20]. □

## 2.2 Computing CBFs using SoS Optimization and Input-Space Sampling

In [21], we presented SOSP 1, a computation procedure based on SoS optimization for computing CBFs. In this subsection, we review the algorithm and comment on its input-space sampling approach.

A multivariate polynomial  $p(x_1, x_2, \dots, x_n) = p(\mathbf{x})$  is an *SoS polynomial* if there exist polynomials  $f_1(\mathbf{x}), \dots, f_m(\mathbf{x})$  such that  $p(\mathbf{x}) = \sum_{i=1}^m f_i^2(\mathbf{x})$ . For example,  $p(x, y) = x^2 - 6xy + 12y^2$  is an SoS polynomial; it can be expressed as  $(x - 3y)^2 + (\sqrt{3}y)^2$ . We denote the set of all SoS polynomials by  $\mathbb{S}$ .

An *SOS optimization Problem* (SOSP), involves finding an  $S \in \mathbb{S}$  such that a linear objective function, whose decision variables are the coefficients of  $S$ , is optimized. The constraints of the problem are linear in the decision variables. A formal definition of an SOSP can be found in the SOSTOOLS user guide (p. 7).

Consider two dynamical systems  $(X_i, \{\mathbf{x}_i^0\}, [u_{min}, u_{max}], f_i, \mathcal{O}, g_i)$ ,  $i = 1, 2$ , with  $u_1$  and  $u_2$  being the scalar inputs of the two systems. Let  $\mathcal{U}^G$  represent a discretized grid for  $u_1$  and  $u_2$ . The grid is formed by dividing the input space  $[u_{min}, u_{max}]$  into a finite number of uniformly spaced intervals, and  $(u_1^i, u_2^j)$  denotes the pair of inputs where  $u_1$  takes the  $i^{th}$  value and  $u_2$  takes the  $j^{th}$  value. In [21], we presented the following SOSP for computing BF's using SoS optimization.

*Definition 2.* SOSP 1, as per [21], is defined by the following equations.

$$\text{Minimize } S(\mathbf{x}_1^0, \mathbf{x}_2^0) \quad (5)$$

subject to:

$$-S(\mathbf{x}_1, \mathbf{x}_2) + [g_1(\mathbf{x}_1) - g_2(\mathbf{x}_2)]^2 \in \mathbb{S}, \quad (6)$$

$$\exists \lambda > 0, \gamma \geq 0 \text{ such that } \forall \mathbf{x}_1, \mathbf{x}_2, u_1^i \in \mathcal{U}^G, u_2^j \in \mathcal{U}^G: \quad (7)$$

$$\begin{aligned} -\frac{\partial S}{\partial \mathbf{x}_1} f_1(\mathbf{x}_1, u_1^i) - \frac{\partial S}{\partial \mathbf{x}_2} f_2(\mathbf{x}_2, u_2^j) - \lambda S(\mathbf{x}_1, \mathbf{x}_2) + \\ \gamma(u_1^i - u_2^j)^2 \in \mathbb{S}. \end{aligned} \quad \blacksquare$$

The CBF  $S$  starts at its maximum value at the pair of initial conditions  $(\mathbf{x}_1^0, \mathbf{x}_2^0)$ , and then decays along various trajectories of the two systems. Thus, along any pair of trajectories, the gap between  $S(\mathbf{x}_1(t), \mathbf{x}_2(t))$  and the Squared Output Difference (SOD)  $[g_1(\mathbf{x}_1(t)) - g_2(\mathbf{x}_2(t))]^2$  is maximum at  $t = 0$ , i.e. at the initial states. To improve the bound on the SOD given by  $S$ , we minimized  $S(\mathbf{x}_1(0), \mathbf{x}_2(0))$  as the objective function of the SOSP.

Eq. (7) enforces the decay condition for a BF, given by Eq. (2), only on the samples  $(u_1^i, u_2^j)$  that comprise the grid  $\mathcal{U}$ . The validity of Eq. (2) on the entire input space can be verified using delta-decidability, as shown in Sec. 5. In Sec. 4, we present an alternative SOSP that enforces Eq. (2) on the entire input space.

Next, we introduce the detailed Markovian potassium-channel model, which is employed as a component in the Iyer-Mazhari-Winslow (IMW) ventricular myocyte model [32].

### 2.3 The Potassium-Channel Subsystem

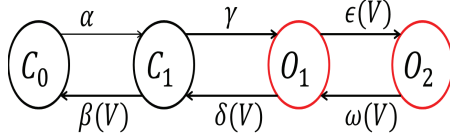


**Figure 2:**  $\Sigma_K$ : the detailed potassium-channel model, corresponding to the ionic current  $I_{K_s}$  in the IMW model.

*Definition 3.* The potassium channel model  $\Sigma_K$  is given by  $(X, X^0, \mathcal{V}, f_K, \mathcal{O}, g_K)$ . A state  $\mathbf{x} \in X \subseteq \mathbb{R}_{\geq 0}^4$  is the occupancy probability distribution over the four states of the voltage-controlled Continuous Time Markov Chain (CTMC) shown in Fig. 2 in the following order of the state labels:  $[C_0, C_1, O_1, O_2]$ . The dynamics  $f_K$  is given by

$$f_K : \dot{\mathbf{x}} = A_K(V) \mathbf{x}, \quad (8)$$

where  $V \in \mathcal{V} \subseteq \mathbb{R}$ , the transmembrane voltage, is the input to the system and  $A_K(V)$  is the  $4 \times 4$  voltage-controlled rate matrix. The off-diagonal entry  $A_K(i, j), i \neq j$ , is the transition rate from state  $\mathbf{x}_j$  to state  $\mathbf{x}_i$ . For example,  $A_K(3, 4) = \omega(V)$ , the transition rate from  $O_2$  to  $O_1$ . The diagonal entry  $A_K(i, i)$  is the negative of the sum of all the outgoing rates from state  $\mathbf{x}_i$ . The transition rates are

$$\begin{aligned} \alpha &= 7.956 \times 10^{-3}, \\ \beta(V) &= 0.216 \times \exp(-0.00002 V), \\ \gamma &= 3.97 \times 10^{-2}, \\ \delta(V) &= (7 \times 10^{-3}) \times \exp(-0.15 V), \\ \epsilon(V) &= (7.67 \times 10^{-3}) \times \exp(0.087 V), \text{ and} \\ \omega(V) &= (3.8 \times 10^{-3}) \times \exp(-0.014 V). \end{aligned}$$

The set of outputs  $\mathcal{O} \subseteq \mathbb{R}_{\geq 0}$  contains the conductance values for the states. Given a state  $\mathbf{x}$ ,  $g_K(\mathbf{x}) \triangleq \mathbf{x}_3 + \mathbf{x}_4$  maps it to its conductance given by the sum of the occupancy probabilities of the states labeled  $O_1$  and  $O_2$ . The system has a single initial condition  $\mathbf{x}_0 = [0.9646, 0.03543, 2.294 \times 10^{-7}, 4.68 \times 10^{-11}] \in X^0$ , as per Table 4 of [32]. ■

Next, we define a one-variable abstraction for  $\Sigma_K$ .

### 2.4 Model-Order Reduction of $\Sigma_K$

The curve fitting-based approach of [2, 13] can be used to identify the following one-variable Hodgkin Huxley (HH)-type approximation for  $\Sigma_K$ .

*Definition 4.* The HH-type abstraction  $\Sigma_H$  is given by  $(Y, Y^0, \mathcal{V}, f_H, \mathcal{O}, g_H)$ . A state  $y \in Y \subseteq \mathbb{R}_{\geq 0}$  denotes the value of an activating (m-type) subunit. The dynamics  $f_H$  is given by

$$f_H : \dot{y} = \alpha_m(V)(1 - y) - \beta_m(V)y, \quad (9)$$

where  $V \in \mathcal{V} \subseteq \mathbb{R}$ , the transmembrane voltage, is the input to the system. The rate functions  $\alpha_m(V)$  and  $\beta_m(V)$ , identified using the two-step curve fitting-based approach of [2,

13], are as follows.

$$\begin{aligned} \alpha_m(V) &= (-1.331 \times 10^{-10})V^4 - (2.466 \times 10^{-7})V^3 \\ &\quad - (9.723 \times 10^{-6})V^2 - 0.0001231V + 0.001049 \end{aligned} \quad (10)$$

$$\begin{aligned} \beta_m(V) &= (4.788 \times 10^{-10})V^6 - (1.547 \times 10^{-8})V^5 \\ &\quad + (1.642 \times 10^{-7})V^4 - (2.85 \times 10^{-6})V^3 \\ &\quad + (6.704 \times 10^{-5})V^2 - (0.0007041)V + 0.003285. \end{aligned} \quad (11)$$

The set of outputs  $\mathcal{O} \subseteq \mathbb{R}_{\geq 0}$  contains the conductance values for the states. Given a state  $\mathbf{y}$ ,  $g_H(\mathbf{y}) \triangleq y$  maps it to its conductance. The system has a single initial condition  $y_0 = 1.32 \times 10^{-5}$ . ■

## 3. CANONICAL CELL MODELS AND COMPOSITIONAL REASONING

In this section, we setup our case study on approximate model-order reduction within feedback loops. We first introduce the voltage subsystem  $\Sigma_C$  representing the cell membrane, which we compose with  $\Sigma_K$  and  $\Sigma_H$  to obtain two *Canonical Cell Models* (CCMs). We then state our compositionality result in terms of the two CCMs, and show how BFs can be used to prove the result.

*Definition 5.* The voltage subsystem  $\Sigma_C$  is a capacitor-like model given by  $(\mathcal{V}, \mathcal{V}^0, \mathcal{O}, f_C, \mathcal{V}, g_C)$ . State  $V \in \mathcal{V} \subseteq \mathbb{R}$  is the voltage. The dynamics of  $\Sigma_C$  is given by

$$f_C : \dot{V} = -G_K(V - E_K) O, \quad (12)$$

where  $G_K = 90.58$  and  $E_K = -35$  mV are the parameters of the model, and  $O \in \mathcal{O} \subseteq \mathbb{R}_{\geq 0}$ , the conductance of the potassium channel, is  $\Sigma_C$ 's input. The system outputs its state, i.e., for  $V \in \mathcal{V}$ ,  $g_C(V) = V$ , and the initial condition is  $V_0 = 0$  mV. ■

As per Eq. (12),  $V_K$  represents the equilibrium for a fixed conductance input. Thus,  $V$  takes values in  $[-35, 0]$ .

In the case of detailed cardiac cell models, such as the IMW model, ion-channel subsystems such as  $\Sigma_K$  and  $\Sigma_H$  take voltage as input from the rest of the model and provide the conductance of the channel as the output. The rest of the model takes the channel conductance as input and outputs the voltage, which is then fed back to the ion-channel subsystems. Next, we define CCMs  $\Sigma_{CK}$  and  $\Sigma_{CH}$  that reflect this feedback-based composition. The models are canonical in the sense that other ion-channel subsystems can be similarly added to obtain a complete IMW model.

*Definition 6.* Systems  $\Sigma_{CK}$  and  $\Sigma_{CH}$  (see Fig. 3) are obtained by performing feedback-composition on the voltage subsystem  $\Sigma_C$  with ion-channel subsystems  $\Sigma_K$  and  $\Sigma_H$ , respectively; i.e.,  $\Sigma_{CK} = \Sigma_C || \Sigma_K$  and  $\Sigma_{CH} = \Sigma_C || \Sigma_H$ . The state spaces, initial conditions, dynamics and outputs are inherited from the subsystems, as explained below. Both  $\Sigma_{CK}$  and  $\Sigma_{CH}$  are autonomous systems and do not receive any external inputs.

A state of  $\Sigma_{CK}$  is given by  $[\mathbf{x}, V_K]^T$ , where  $\mathbf{x}$  is a state of  $\Sigma_K$  and  $V_K$  is a state of  $\Sigma_C$ . The subscript  $K$  in  $V_K$  is used to denote the copy of  $\Sigma_C$  composed with  $\Sigma_K$ . The system dynamics are given by Eqs. (8) and (12). The output is given by  $[g_K(\mathbf{x}), V_K]^T$ . The initial condition is the pair of the initial conditions of  $\Sigma_K$  and  $\Sigma_C$ .

A state of  $\Sigma_{CH}$  is given by  $[y, V_H]^T$ , where  $y$  denotes a state of  $\Sigma_H$  and  $V_H$  denotes a state of  $\Sigma_C$ . The subscript  $H$  in  $V_H$  is used to denote the copy of  $\Sigma_C$  composed with  $\Sigma_H$ . The system dynamics are given by Eqs. (9) and (12). The output is given by  $[g_H(y), V_H]^T$ . The initial condition is the pair of the initial conditions of  $\Sigma_H$  and  $\Sigma_C$ . ■

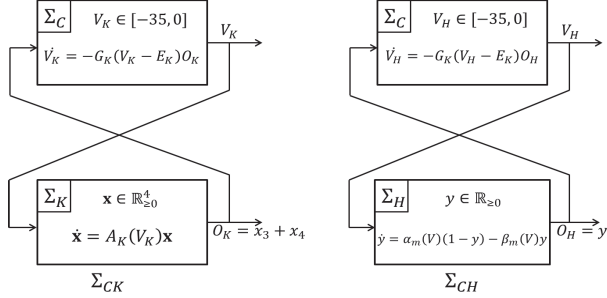
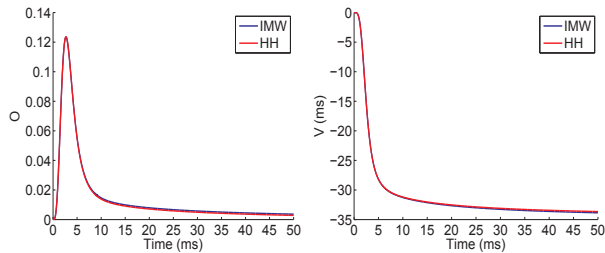


**Figure 3:**  $\Sigma_{CK}$  and  $\Sigma_{CH}$ : ion-channel subsystems  $\Sigma_K$  and  $\Sigma_H$  are feedback-composed with  $\Sigma_C$ , which represents the cell membrane.  $\Sigma_{CH}$  is obtained by i) identifying the one-variable abstraction  $\Sigma_H$  of  $\Sigma_K$  using the curve-fitting procedure given in [2, 13]; and ii) substituting  $\Sigma_H$  for the detailed model  $\Sigma_K$  within  $\Sigma_{CK}$ .

When  $\Sigma_K$  in  $\Sigma_{CK}$  is replaced by  $\Sigma_H$  to obtain  $\Sigma_{CH}$ , the behaviors of the composite CCMs might diverge. This is due to the feedback composition that tends to amplify deviations in the outputs of either of the subsystems. Fig. 4 shows a pair of trajectories of  $\Sigma_{CK}$  and  $\Sigma_{CH}$  that start from nominal initial conditions. The goal of the paper is to compute BFs that prove that the composite CCMs are indeed approximately equivalent, i.e., the following statement holds.



(a)  $O_K(t)$  and  $O_H(t)$  of  $\Sigma_{CK}$  and  $\Sigma_{CH}$  respectively. (b)  $V_K(t)$  and  $V_H(t)$  of  $\Sigma_{CK}$  and  $\Sigma_{CH}$  respectively.

**Figure 4:** Simulations of  $\Sigma_{CK}$  and  $\Sigma_{CH}$ : when  $\Sigma_K$  is replaced by  $\Sigma_H$ , feedback composition tends to accumulate error incurred due to the abstract component. The mean L1 errors:  $O_{K_s} : 1.1786 \times 10^{-4}$ ,  $V : 0.2002$  mV.

*Compositionality Result:* There exists a BF  $S$  between  $\Sigma_{CK}$  and  $\Sigma_{CH}$  that renders the two CCMs to be approximately equivalent as characterized by Theorem 1.

$S$  is computed compositionally as follows. First, the components  $\Sigma_K$  and  $\Sigma_H$  are proved to be approximately equivalent by computing a BF  $S_{KH}$  between the two systems. Then, the context  $\Sigma_C$  is proved to be robust to input deviations by computing a BF  $S_C$  for it. The computation procedure ensures that the prerequisite small-gain condition

is satisfied by  $S_{KH}$  and  $S_C$ , thereby enabling the application of Theorem 2; this results in a BF  $S$  between  $\Sigma_{CK}$  and  $\Sigma_{CH}$ . Next, we describe **BFCOMP** and apply it for computing  $S_{KH}$  and  $S_C$  in the following sections.

## 4. COMPUTING BFs USING SoS OPTIMIZATION

In this section, we describe SOSP 2, an SOSP formulation that can be used to compute BFs. SOSP 2, in contrast to SOSP 1, which was reviewed in Section 2.2, exhaustively covers the input-space. First, we present the problem formulation and then we show that the solutions are indeed BFs.

We assume that the input spaces are described using sets, such as  $\mathcal{U} = \{u \in \mathbb{R} : \rho(u) \geq 0\}$ , where  $\rho(u)$  is called a *descriptor function*. For example,  $\rho(u) = (u - u_{min})(u_{max} - u)$  describes the input-space  $\mathcal{U} = [u_{min}, u_{max}]$ . We denote the components of the state vectors as  $\mathbf{x}_1 = [x_{11}, x_{12}, \dots, x_{1n_1}]$  and  $\mathbf{x}_2 = [x_{21}, x_{22}, \dots, x_{2n_2}]$ . Each of these components take values in a closed interval, i.e.  $x_{11} \in [\underline{x}_{11}, \overline{x}_{11}]$ ,  $\dots$ ,  $x_{1n_1} \in [\underline{x}_{1n_1}, \overline{x}_{1n_1}]$  and  $x_{21} \in [\underline{x}_{21}, \overline{x}_{21}]$ ,  $\dots$ ,  $x_{2n_2} \in [\underline{x}_{2n_2}, \overline{x}_{2n_2}]$ . We introduce vectors of polynomials  $\tau_1$  and  $\tau_2$  as descriptor functions of the state vectors:

$$\tau_i(\mathbf{x}_i) = \begin{bmatrix} (x_{i1} - \underline{x}_{i1})(\overline{x}_{i1} - x_{i1}) \\ \vdots \\ (x_{in_i} - \underline{x}_{in_i})(\overline{x}_{in_i} - x_{in_i}) \end{bmatrix}, i = 1, 2. \quad (13)$$

*Definition 7.* Consider two dynamical systems  $\Sigma_i = (X_i, \{\mathbf{x}_i^0\}, [u_{min}, u_{max}], f_i, \mathcal{O}, g_i)$ ,  $i = 1, 2$ . SOSP 2 is given by the following equations.

$$\text{Minimize } S(\mathbf{x}_1^0, \mathbf{x}_2^0) \quad (14)$$

subject to:

$$S(\mathbf{x}_1, \mathbf{x}_2) - [g_1(\mathbf{x}_1) - g_2(\mathbf{x}_2)]^2 \in \mathbb{S}, \quad (15)$$

$$\forall u_i \in [u_{min}, u_{max}], x_{ij} \in [\underline{x}_{ij}, \overline{x}_{ij}], i = 1, 2, j = 1, \dots, n_i,$$

$\exists \lambda > 0, \gamma \geq 0, \sigma_1(\mathbf{x}_1, u_1) \in \mathbb{S}, \sigma_2(\mathbf{x}_2, u_2) \in \mathbb{S}$ , and vectors of SoS polynomials  $\sigma_3(\mathbf{x}_1, u_1)$  and  $\sigma_4(\mathbf{x}_2, u_2)$  such that :

$$\begin{aligned} & - \frac{\partial S}{\partial \mathbf{x}_1} f_1(\mathbf{x}_1, u_1) - \frac{\partial S}{\partial \mathbf{x}_2} f_2(\mathbf{x}_2, u_2) - \lambda S(\mathbf{x}_1, \mathbf{x}_2) + \\ & \gamma(u_1 - u_2)^2 - \sigma_1(\mathbf{x}_1, u_1)\rho(u_1) - \sigma_2(\mathbf{x}_2, u_2)\rho(u_2) - \\ & \sigma_3(\mathbf{x}_1, u_1)\tau_1(\mathbf{x}_1) - \sigma_4(\mathbf{x}_2, u_2)\tau_2(\mathbf{x}_2) \in \mathbb{S}. \end{aligned} \quad (16)$$

Next, we show that the feasible solutions of SOSP 2 are indeed BFs for the two systems.

*Theorem 3.* Consider a feasible solution,  $(S, \sigma_1, \sigma_2, \sigma_3, \sigma_4, \lambda, \gamma)$ , of the SOSP 2.  $S$  satisfies Eqs. (1) and (2), and thus is a BF between  $\Sigma_1$  and  $\Sigma_2$ .

**PROOF.**  $S$ , from a feasible solution  $(S, \sigma_1, \sigma_2, \sigma_3, \sigma_4, \lambda, \gamma)$ , satisfies Eq. (15):

$$\forall \mathbf{x}_1, \mathbf{x}_2 : S(\mathbf{x}_1, \mathbf{x}_2) - [g_1(\mathbf{x}_1) - g_2(\mathbf{x}_2)]^2 \in \mathbb{S}.$$

As an SoS polynomial is always non-negative, we get

$$S(\mathbf{x}_1, \mathbf{x}_2) - [g_1(\mathbf{x}_1) - g_2(\mathbf{x}_2)]^2 \geq 0,$$

which implies  $[g_1(\mathbf{x}_1) - g_2(\mathbf{x}_2)]^2 \leq S(\mathbf{x}_1, \mathbf{x}_2)$ ,  $S$  satisfies Eq. (1).

A feasible solution satisfies Eq. (16):

$$\begin{aligned}
& -\frac{\partial S}{\partial \mathbf{x}_1} f_1(\mathbf{x}_1, u_1) - \frac{\partial S}{\partial \mathbf{x}_2} f_2(\mathbf{x}_2, u_2) - \lambda S(\mathbf{x}_1, \mathbf{x}_2) + \\
& \gamma(u_1 - u_2)^2 - \sigma_1(\mathbf{x}_1, u_1)\rho(u_1) - \sigma_2(\mathbf{x}_2, u_2)\rho(u_2) - \\
& \sigma_3(\mathbf{x}_1, u_1)\tau_1(\mathbf{x}_1) - \sigma_4(\mathbf{x}_2, u_2)\tau_2(\mathbf{x}_2) \in \mathbb{S}.
\end{aligned}$$

Non-negativity of SoS polynomials leads to

$$\begin{aligned}
& -\frac{\partial S}{\partial \mathbf{x}_1} f_1(\mathbf{x}_1, u_1) - \frac{\partial S}{\partial \mathbf{x}_2} f_2(\mathbf{x}_2, u_2) - \sigma_1(\mathbf{x}_1, u_1)\rho(u_1) \\
& - \sigma_2(\mathbf{x}_2, u_2)\rho(u_2) - \sigma_3(\mathbf{x}_1, u_1)\tau_1(\mathbf{x}_1) - \sigma_4(\mathbf{x}_2, u_2)\tau_2(\mathbf{x}_2) \\
& \geq \lambda S(\mathbf{x}_1, \mathbf{x}_2) - \gamma(u_1 - u_2)^2.
\end{aligned}$$

Multiplying both sides by -1 and then reversing the inequality, we get

$$\begin{aligned}
& \frac{\partial S}{\partial \mathbf{x}_1} f_1(\mathbf{x}_1, u_1) + \frac{\partial S}{\partial \mathbf{x}_2} f_2(\mathbf{x}_2, u_2) + \sigma_1(\mathbf{x}_1, u_1)\rho(u_1) \\
& + \sigma_2(\mathbf{x}_2, u_2)\rho(u_2) + \sigma_3(\mathbf{x}_1, u_1)\tau_1(\mathbf{x}_1) + \sigma_4(\mathbf{x}_2, u_2)\tau_2(\mathbf{x}_2) \\
& \leq -\lambda S(\mathbf{x}_1, \mathbf{x}_2) + \gamma(u_1 - u_2)^2.
\end{aligned}$$

As  $\sigma_1(\mathbf{x}_1, u_1)\rho(u_1) + \sigma_2(\mathbf{x}_2, u_2)\rho(u_2) + \sigma_3(\mathbf{x}_1, u_1)\tau_1(\mathbf{x}_1) + \sigma_4(\mathbf{x}_2, u_2)\tau_2(\mathbf{x}_2)$  is always non-negative, we can eliminate the sum and still retain the inequality to get

$$\begin{aligned}
\frac{\partial S}{\partial \mathbf{x}_1} f_1(\mathbf{x}_1, u_1) + \frac{\partial S}{\partial \mathbf{x}_2} f_2(\mathbf{x}_2, u_2) & \leq -\lambda S(\mathbf{x}_1, \mathbf{x}_2) + \\
& \gamma(u_1 - u_2)^2.
\end{aligned}$$

□

## 5. VALIDATING SOSP 1 CBFs USING DELTA-DECIDABILITY

Consider the two dynamical systems  $(X_i, \{\mathbf{x}_i^0\}, [u_{min}, u_{max}], f_i, O, g_i)$ ,  $i = 1, 2$ . Let  $S$ , parameterized by  $\lambda$  and  $\gamma$ , be a CBF, which can be obtained by solving SOSP 1, see Def. 2. A valid solution of SOSP 1 satisfies Eq. (2) over the input grid  $\mathcal{U}^G$  that is used in SOSP 1. The focus of this section is to validate if  $S$  satisfies Eq. (2) over all the states and inputs, and thus is a BF for the two systems. For this purpose, we use *dReal* [7], which implements delta-decidability, to validate  $S$ . Consider the function  $\psi$ .

$$\begin{aligned}
\psi(\mathbf{x}_1, \mathbf{x}_2, u_1, u_2) & \triangleq -\frac{\partial S}{\partial \mathbf{x}_1} f_1(\mathbf{x}_1, u_1) - \frac{\partial S}{\partial \mathbf{x}_2} f_2(\mathbf{x}_2, u_2) \\
& - \lambda S(\mathbf{x}_1, \mathbf{x}_2) + \gamma(u_1 - u_2)^2.
\end{aligned}$$

If  $S$  satisfies Eq. (2) over the entire state and input space, then the following SMT formula must be unsatisfiable:

$$\exists \mathbf{x}_1, \mathbf{x}_2, u_1, u_2 : \psi(\mathbf{x}_1, \mathbf{x}_2, u_1, u_2) < 0 \quad (17)$$

Delta-decidability, which involves relaxing  $\psi$  by a parameter  $\delta > 0$ , can be used to check if Eq. (17) is indeed unsatisfiable. The open-source tool *dReal* implements  $\delta$ -decision procedures and can be used for our problem. A decision procedure is said to be  $\delta$ -complete if for any SMT formula, it returns either *unsat*, if the formula is unsatisfiable, or returns  $\delta$ -sat, if the formula's  $\delta$ -relaxation is satisfiable, see [7, 5, 6] for a formal definition.

When Eq. (17) is presented to *dReal*, with a pre-determined  $\delta$ , three possibilities, which are illustrated in Fig. 5, arise. We discuss each of them next.

*Case A*, *dReal* returns *unsat*: Eq. (17) is unsatisfiable, and therefore  $S$  is a valid BF. Delta-relaxation ensures a stronger

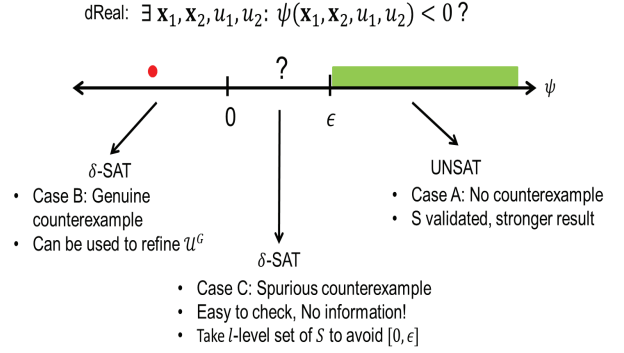


Figure 5: Validating SOSP 1-based CBFs using *dReal*.

result, we may claim that  $\psi \geq \epsilon$ , where  $\epsilon$  is a function of  $\delta$  and other internal parameters of *dReal*.

*Case B*, *dReal* returns  $\delta$ -sat, with a counterexample, where  $\psi < 0$ . The tuple of states and inputs that is returned as the counterexample contains an input pair, where  $S$  fails to satisfy Eq. (2). The input pair is then used to refine  $\mathcal{U}^G$  and SOSP 1 is repeated; Eq. (7), which represents a family of inequalities, is instantiated over  $\mathcal{U}^G$ , as well as the input pair from the counterexample.

*Case C*, *dReal* returns  $\delta$ -sat, with a counterexample, where  $\psi \geq 0$ . This possibility arises due to the delta-relaxation. The formula  $\psi$  evaluates to a very small value in the range  $[0, \epsilon]$ . The counterexample is spurious and does not provide any information about  $S$ . Thus, we present a workaround to avoid this case.

To avoid Case C, we filter the domain of the state variables  $\mathbf{x}_1$  and  $\mathbf{x}_2$  in Eq. (17) to eliminate the pairs of states that contribute to the spurious counterexamples. Specifically, we validate the CBF  $S$  only on, and outside its  $l$ -level set. Eq. (17) is modified as

$$\exists \mathbf{x}_1, \mathbf{x}_2, u_1, u_2 : (S(\mathbf{x}_1, \mathbf{x}_2) \geq l) \wedge (\psi(\mathbf{x}_1, \mathbf{x}_2, u_1, u_2) < 0) \quad (18)$$

The intuition behind level-set-based filtering of the domain is as follows. The function  $\psi$  goes to 0 when the states and the inputs go to 0. Also,  $\psi$  bounds the derivative of  $S$  with respect to time. The time-derivative of  $S$  takes very low values near the origin of the state-space, as the the origin is an equilibrium for our systems. Fig. 7 illustrates this property. When the inputs to the subsystem are held constant, the derivative of a BF becomes very low as the trajectories decay to the origin, which is a stable equilibrium. Thus, the derivative of  $S$  with respect to time, and consequently  $\psi$ , will have relatively larger values outside the  $l$ -level set of  $S$ .

The parameter  $l$  may be tuned till we avoid Case C completely and cover as many states as possible. Starting from an aggressive small value of  $l \geq 0$ , it may be incremented in small steps till Case C is completely avoided.

Our level-set-based approach can be justified as follows. We define the exterior of the  $l$ -level set of  $S$  as:  $S^{\geq l} \triangleq \{(\mathbf{x}_1, \mathbf{x}_2) | S(\mathbf{x}_1, \mathbf{x}_2) \geq 0\}$ . Validating Eq. (17) over  $S^{\geq l}$  ensures that Eq. (1) and Eq. (2) are satisfied for all states within  $S^{\geq l}$ . In a practical setting, where we want to establish IOS between two systems, the sets of initial conditions become important. Given the decaying nature of a BF, the maximum value of the BF over a given pairing of the initial states is the best bound on the SOD that the BF can

provide. Approximate bisimilarity of two systems can be established by minimizing the maximum value of the BF over all pairings of the initial states. For a given CBF, if this value is greater than the level set  $l$ , at which the CBF is validated, then the CBF can be used to provide practical bounds on the SOD.

CBFs validated using the level-set-based approach also enable compositionality arguments, albeit in a weaker setting. To this end, we state the following proposition.

*Proposition 1.* Let  $\Sigma_i = (\mathcal{X}_i, \mathcal{X}_i^0, \mathcal{U}_i, f_i, \mathcal{O}_i, g_i)$ ,  $i = 1, 2, A, B$ , be dynamical systems such that  $\mathcal{U}_1 = \mathcal{O}_A$ ,  $\mathcal{U}_A = \mathcal{O}_1$ ,  $\mathcal{U}_2 = \mathcal{O}_B$  and  $\mathcal{U}_B = \mathcal{O}_2$ . Let  $S_{12}$ , parameterized by  $\lambda_{12}$  and  $\gamma_{12}$ , be a BF between  $\Sigma_1$  and  $\Sigma_2$  in  $S_{12}^{\geq l_1}$ . Let  $S_{AB}$ , parameterized by  $\lambda_{AB}$  and  $\gamma_{AB}$ , be a BF between  $\Sigma_A$  and  $\Sigma_B$  in  $S_{AB}^{\geq l_2}$ .

Let  $\Sigma_{A1} = \Sigma_A || \Sigma_1$  and  $\Sigma_{B2} = \Sigma_B || \Sigma_2$ . If the *small gain condition* (SGC)  $\frac{\gamma_{AB}\gamma_{12}}{\lambda_{AB}\lambda_{12}} < 1$  is met, then a BF  $S$  between  $\Sigma_{A1}$  and  $\Sigma_{B2}$ , which satisfies Eq. (1) and Eq. (2) over  $S_{12}^{\geq l_1} \times S_{AB}^{\geq l_2}$ , can be constructed as follows.

$$S(\mathbf{x}_{A1}, \mathbf{x}_{B2}) = \alpha_1 S_{AB}(\mathbf{x}_A, \mathbf{x}_B) + \alpha_2 S_{12}(\mathbf{x}_1, \mathbf{x}_2)$$

where  $\mathbf{x}_{A1} = [\mathbf{x}_A, \mathbf{x}_1]^T$  and  $\mathbf{x}_{B2} = [\mathbf{x}_B, \mathbf{x}_2]^T$  and the constants  $\alpha_1$  and  $\alpha_2$  are as per Theorem 2.

PROOF. See supplementary document [20].  $\square$

## 6. RESULTS

In this section, we elaborate on computing the BFs  $S_{KH}$ ,  $S_C$ , and the composed BF  $S$  between  $\Sigma_{CK}$  and  $\Sigma_{CH}$  using **BFComp**. The BFs computed using SOSP 1 and SOSP 2 are then visualized along pairs of trajectories obtained by feeding constant-input signals to the corresponding systems.

### 6.1 Computing $S_{KH}$ and $S_C$ using SOSP 2

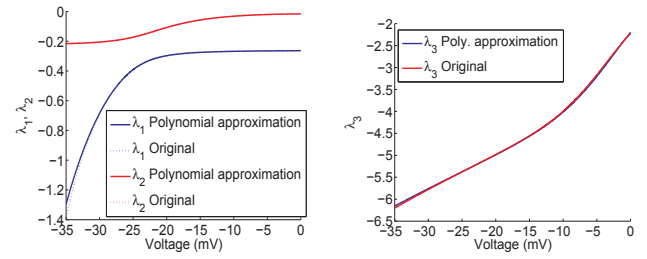
Automated solvers, such as MATLAB SOSTOOLS [26], which can be used to solve SOSP 2, have the following restriction: only polynomial vector fields, denoted by  $f_i(\mathbf{x}_i, u_i)$ ,  $i = 1, 2$  in Eq. (16), can be specified. In other words,  $f_i$  must be a polynomial function of  $\mathbf{x}_i$  and  $u_i$ .

The potassium-channel subsystem  $\Sigma_K$  does not satisfy the above-mentioned requirement. The dynamics, see Eq. (8), is specified by  $\dot{\mathbf{x}} = A_K(V)\mathbf{x}$ , where  $\mathbf{x}$  is the occupancy-probability vector and  $A_K(V)$  is the rate matrix, whose entries are *exponential functions of the input membrane potential*  $V$ , see Defn. 3. Thus, the dynamics of  $\Sigma_K$  are not polynomial in the input.

As a workaround, we transformed the rate matrix  $A_K(V)$  to an approximately equivalent matrix  $A_K^p(V)$  by fitting the entries of  $A$  with polynomial functions using MATLAB *cftool* [22]. The polynomial approximations of the voltage-dependent rate functions, denoted by the superscript  $p$  are as follows.

$$\begin{aligned} \beta^p(V) &= -(4.322 \times 10^{-6})V + 0.216, \\ \delta^p(V) &= (2.125 \times 10^{-10})V^6 - (9.322 \times 10^{-9})V^5 + \\ &\quad (8.964 \times 10^{-8})V^4 - (1.716 \times 10^{-6})V^3 + \\ &\quad (8.87 \times 10^{-5})V^2 - 0.001284V + 0.006744, \\ \epsilon^p(V) &= (4.435 \times 10^{-9})V^4 + (5.191 \times 10^{-7})V^3 + \\ &\quad (2.539 \times 10^{-5})V^2 + (0.0006507)V + 0.007652, \text{ and} \\ \omega^p(V) &= (3.771 \times 10^{-7})V - (5.415 \times 10^{-5})V + 0.0038. \end{aligned}$$

Polynomial approximations can be justified as follows. We show that the difference in the eigenvalues of  $A_K(V)$  and  $A_K^p(V)$ , which controls the difference between corresponding trajectories of the two systems, is negligible for  $V \in [-35, 0]$ . Moreover, the difference can be bounded after the polynomial curve fitting is completed. The resulting error between the trajectories can then be used to relax the bound on SOD provided by Theorem 1. Note that, in general, Weierstrass Approximation theorem [14] allows us to find polynomial approximations of the continuous exponential functions, like  $\beta(V)$ ,  $\delta(V)$ ,  $\epsilon(V)$ , and  $\omega(V)$ , to any degree of accuracy for  $V \in [-35, 0]$ . Once the polynomial approximations have been identified, the Bauer-Fike theorem [3] can be used to bound the corresponding error in the eigenvalues. For our polynomial approximations, Fig. 6 plots the spectrum of the two matrices  $A_K(V)$  and  $A_K^p(V)$  as a function of  $V$ . Only three eigenvalues are plotted as one of the four state-variables of  $\Sigma_K$  can be eliminated, as they sum to 1, resulting in a  $3 \times 3$  rate matrix.



(a) First and second eigenvalues: mean L1 errors are 0.005 and  $4.45 \times 10^{-4}$ . (b) Third eigenvalue, scale of y-axis is  $10^{-3}$ . Mean L1 error is  $1.68 \times 10^{-5}$ .

Figure 6: Spectrum of  $A_K$  and  $A_K^p$ .

Computing  $S_{KH}$  and  $S_C$  using SOSP 2 begins with declaring the form of the BFs. We chose ellipsoidal forms using the `ossosvar` function provided by SOSTOOLS:  $S_{KH}(\mathbf{x}, \mathbf{y}) = [\mathbf{x}, \mathbf{y}] \cdot Q_{KH} \cdot [\mathbf{x}, \mathbf{y}]^T$  and  $S_C(V_K, V_H) = [V_K, V_H] \cdot Q_C \cdot [V_K, V_H]^T$ . Variables  $\mathbf{x}, \mathbf{y}, V_K$ , and  $V_H$  are declared using the `pvar` polynomial variable toolbox. The coefficients of the BFs, which form the decision variables of the SOSPs, are contained in the positive semidefinite matrices  $Q_{KH}$  ( $4 \times 4$ ) and  $Q_C$  ( $2 \times 2$ ). We chose ellipsoidal forms, using the `ossosvar`, for the  $\sigma(\cdot, \cdot)$  functions that strengthen the decay requirement in Eq. (16) of Defn. 7. The descriptor functions were obtained from the definitions  $\Sigma_K$ ,  $\Sigma_H$  and  $\Sigma_C$ .

SOSP2 was implemented in MATLAB R2013a, SOSTOOLS 2.04 [26] on an Intel Core i7-4770K 3.5 GHz CPU with 32 GB of memory. For  $S_{KH}$ , SOSTOOLS terminated in 5.95 seconds with the following flags: *feas ratio* = 0.3147, *pinf* = *dinf* = 0, *numerr* = 1. For  $S_C$ , SOSTOOLS terminated in 5.95 seconds with the following flags: *feas ratio* = 1.03, *pinf* = *dinf* = *numerr* = 0.

### 6.2 Computing $S_{KH}$ and $S_C$ using SOSP 1 and dReal

The details of implementing SOSP 1 in MATLAB SOSTOOLS can be found in Sec. 3 of [21]. We provide details on dReal-based validation of the CBFs.

For  $S_{KH}$ ,  $\mathcal{V} = [-35, -25, -15, -5, 0]$ .  $\mathcal{V} \times \mathcal{V}$  was used as the input grid to compute the CBF  $S_{KH}$  using SOSP 1.  $S_{KH}$  was parameterized by  $\lambda_{KH} = 0.001$  and  $\gamma_{KH} = 0.0001$ . The CBF was validated as per Sec. 5; Eq. (18) was proved

to be *unsat* in dReal by choosing  $l = 0.001$ .

For  $S_C$ , we considered  $\mathcal{O} \times \mathcal{O}$  as the input grid, where  $\mathcal{O} = [0.1, 0.2, 0.3, 0.4, 0.5, 0.6, 0.7, 0.8, 0.9, 1]$ .  $S_C$  was parameterized by  $\lambda_C = 0.001$  and  $\gamma_C = 0.0001$ . The CBF was validated as per Sec. 5; Eq. (18) was proved to be *unsat* in dReal by choosing  $l = 1$ .

The validation was implemented using dReal's version 2.14.08-linux [7] on an Intel Core i7-4770K 3.5 GHz CPU with 32 GB of memory. The running time was 416 minutes and 58.64 seconds for  $S_{KH}$  and 7 seconds for  $S_C$ .

### 6.3 Composing $S_{KH}$ and $S_C$ using the Small-Gain Theorem

The parameters of  $S_{KH}$  and  $S_C$  satisfy the SGC condition of Theorem 2, as  $\frac{\gamma_{KH}\gamma_C}{\lambda_{KH}\lambda_C} = 0.01 < 1$  in both SOSP 1 and SOSP 2. Applying Theorem 2, we linearly composed  $S_{KH}$  and  $S_C$  to obtain  $S = \alpha_1 S_{KH} + \alpha_2 S_C$ , where  $\alpha_1, \alpha_2 = 1$ .  $S$  is a BF between the composite systems  $\Sigma_{CK}$  and  $\Sigma_{CH}$ . As per Theorem 2 of [1], the parameter  $\lambda$  of  $S$  is given by

$$\lambda = \min \left( \frac{\alpha_1 \lambda_{KH} - \alpha_2 \gamma_C}{\alpha_1}, \frac{\alpha_2 \lambda_C - \alpha_1 \gamma_{KH}}{\alpha_2} \right) = 0.0009.$$

### 6.4 Visualizing the BFs

Empirical validation of the BFs is provided by plotting them in 2D along the time axis. As the time proceeds in the same manner in both systems, the corresponding BF is plotted for the pair of states occurring at the same time along the trajectories of the systems. The SOD observed for the pair of states is also plotted in the same graph. The resulting plots show that the BFs bound the SOD and decay in time along the pairs of trajectories, as per Theorem 1.

Figs. 7 (a) - (c) show  $S_{KH}$  plotted along three pairs of trajectories of  $\Sigma_K$  and  $\Sigma_H$ . Each pair was generated by supplying a pair of constant voltage signals ( $V_1(t), V_2(t)$ ) as inputs to  $\Sigma_K$  and  $\Sigma_H$ , respectively. The two subsystems were initialized as per Defs. 3 and 4, and simulated using MATLAB's *ODE45* solver.  $S_{KH}$  was then evaluated along the resulting pair of trajectories after shifting the origin to the equilibrium defined by ( $V_1(t), V_2(t)$ ). In two cases,  $S_{KH}$  computed using SOSP 2 provides slightly better error bound than that of using SOSP 1.

$S_C$  characterizes the ability of  $\Sigma_C$  to tolerate small changes in the input signals. In the composite systems  $\Sigma_{CK}$  and  $\Sigma_{CH}$ , these signals are provided by subsystems  $\Sigma_K$  and  $\Sigma_H$ , and thus vary slightly due to the fitting errors incurred by the model-order reduction as described in Sec.2.4.

$S_C$  is plotted in Figs. 7 (d) - (f) along three pairs of trajectories of  $\Sigma_C$ . Each pair of trajectories was generated by supplying constant conductance (input) signals ( $O_1(t), O_2(t)$ ).  $\Sigma_C$  was initialized at 0 mV and simulated using the Euler method.  $S_C$  was evaluated along the resulting trajectories after shifting the origin to the equilibrium, -35 mV ( $E_K$ ). We observed that  $S_C$  computed using SOSP 1 gives a tighter SOD bound compared to SOSP 2.

CCMs  $\Sigma_{CK}$  and  $\Sigma_{CH}$  are autonomous dynamical systems and do not receive any external inputs. To visualize the composite BF  $S$ , we simulated  $\Sigma_{CK}$  and  $\Sigma_{CH}$  using the Euler method for different initial conditions. Fig. 4 plots the trajectories obtained from these simulations. The corresponding conductance traces of Fig. 4(a) and the voltage traces of Fig. 4(b) empirically validate that the composed models are approximately equivalent as predicted by Theorem 2. BF  $S$

along this pair, and two other pairs of trajectories is plotted in Fig. 7 (g) - (i). The value of  $S$  is dominated by the value of  $S_C$ , as it bounds the squared difference of voltages and is much larger than  $S_{KH}$ , which bounds differences in probabilities. This is reasonable as voltage is the primary entity of interest when analyzing excitable cells. One could scale subsystem  $\Sigma_C$  such that its output lies in  $[0, 1]$  and is thus comparable to the outputs of  $\Sigma_K$  and  $\Sigma_H$ . In all three cases,  $S$  computed using SOSP 1 performs much better than the one computed using SOSP 2.

## 7. RELATED WORK

Initial work on computing BFs, [8, 9, 10, 1, 15, 17], depended primarily on SOS optimization. SOS optimization has also played a crucial role in enabling the automated computation of other Lyapunov-like functions, such as Barrier Certificates [25, 24] and discrepancy functions [4, 12]. In [25, 17], the authors employ an SOSP 2-like approach, which is based on the S-Procedure of [33] and entails strengthening the Lyapunov-like inequalities over the region-of-interest in the state and input spaces.

Despite the success of the above-mentioned approaches, SOS-optimization-based techniques suffer from various drawbacks, such as numerical errors and choosing the forms of the unknown polynomials, which may be crucial for getting good SOD bounds. The *simulation-based approach* to analyzing stability of dynamical systems in [16], which is closely related to our work, addresses some of these issues. Simulation traces of a given dynamical system are used to compute so-called Candidate Lyapunov Functions (CLFs). The authors then use an SMT-based ensemble of tools, which includes dReal, to validate the decay requirements over level sets of the CLF. The **BFComp** framework differs from the work of [16] in three ways. Firstly, we focus on BFs that characterize IOS of dynamical systems, whereas the authors focus on Lyapunov stability in [16]. Secondly, as shown in our case study, our framework places emphasis on SOD to enable bounding the error that is incurred when a detailed subsystem is replaced by an abstraction within a feedback loop. Lastly, our framework is completely based on Sum-of-Square optimization, whereas the authors use a Linear Programming (LP)-based approach to computing the CLFs.

**BFComp** builds upon our previous work of [21], which proposed SOSP1, in several ways. SOSP1, as a standalone BF-computation technique, suffers from the following limitation: the decay condition of Eq. (2) is enforced only on a grid-based discretized input-space. Therefore, SOSP1 cannot be used to establish incremental input-to-output stability for a continuum of input values. **BFComp** overcomes this limitation in two ways. First, SOSP2, which covers the input space exhaustively, is applied. If the resulting BF fails to provide satisfactory bounds on the SOD, then SOSP1 is used to compute CBFs. The CBFs are then validated using dReal-based delta reachability. In summary, **BFComp** overcomes SOSP1's limitation of input-space discretization, as well as attempts to provide relatively tight SOD bounds.

*LP-based computation* of Lyapunov-like functions is a promising alternative to SOS optimization. In [28, 27], the authors present LP formulations, based on Handelman representations of polynomials, to compute Lyapunov functions. Consequently, the computation avoids semi-definite programming, which enables SOS optimization, and is therefore more robust to numerical errors. Incorporating such LP-based ap-

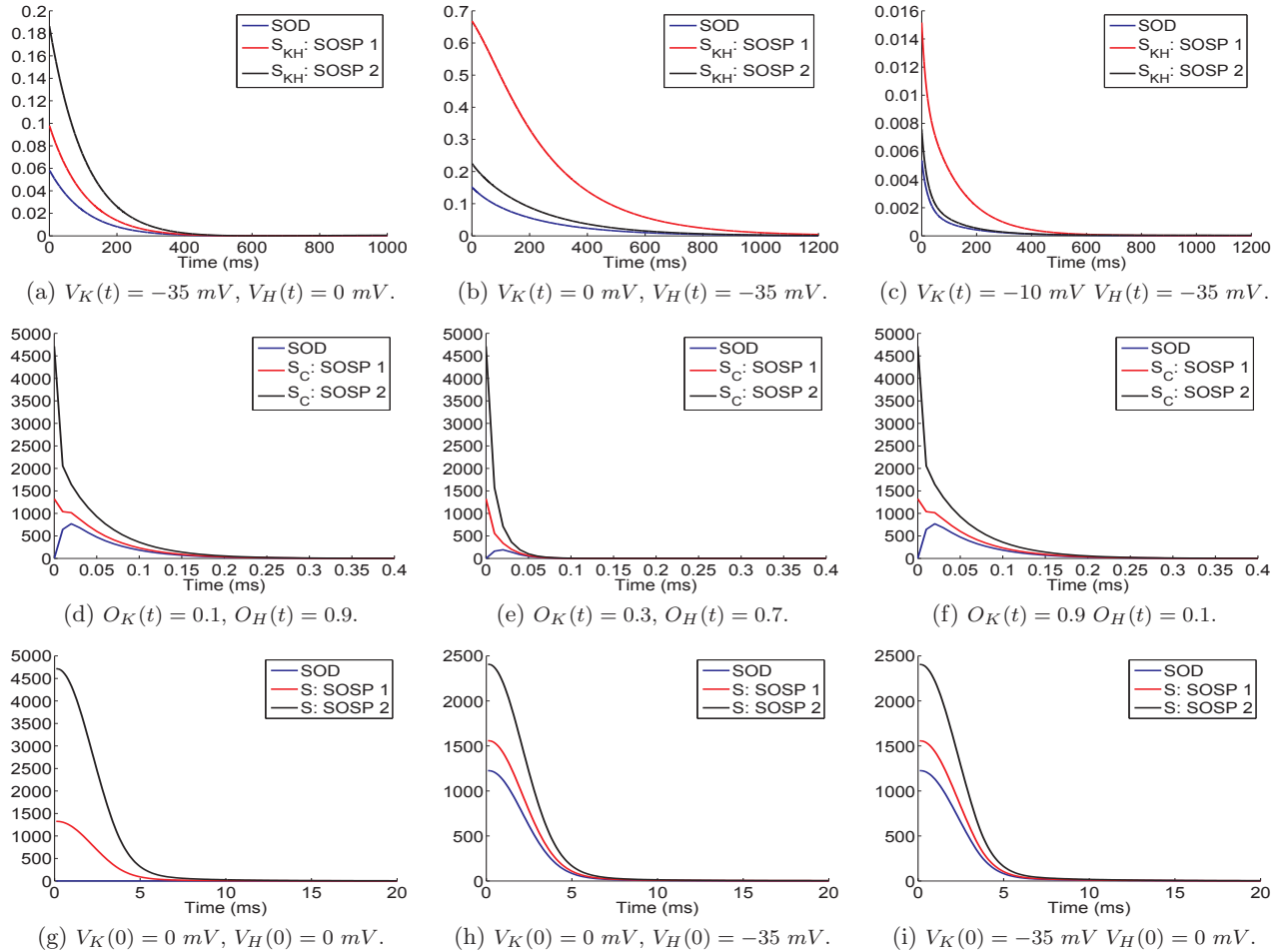


**Figure 7:** BFs  $S_{KH}$ ,  $S_C$ ,  $S$ , and their corresponding SOD plotted along trajectories of the respective systems. In subfigures (a) - (c),  $S_{KH}$  and SOD are plotted along three pairs of trajectories of  $\Sigma_K$  and  $\Sigma_H$  generated using constant voltage (input) signals. In subfigures (d) - (f),  $S_C$  and SOD are plotted along three pairs of trajectories of  $\Sigma_C$  generated using constant conductance (input) signals. In subfigures (g) - (i), the composed BF  $S$  and SOD are plotted along three pairs of trajectories of  $\Sigma_{CK}$  and  $\Sigma_{CH}$  generated using different initial conditions. In all three cases, the BFs upper bound the SOD and decay along the trajectories.

proaches into our framework is part of the future work.

## 8. CONCLUSIONS

We presented *BFComp*, an automated framework based on SOS optimization and  $\delta$ -decidability over the reals for computing BFs that characterize IOS of dynamical systems and provide reasonable bounds on the SOD between the systems. We applied *BFComp* to compute BFs that appeal to a small-gain theorem, thereby compositionally showing that a detailed four-variable potassium-channel model can be safely replaced by an approximately equivalent one-variable abstraction within a feedback-composed system.

As future work, we plan to incorporate the SOD bound explicitly in *BFComp*, as a feedback that enables iterative improvement of the BFs. We will also investigate the LP-based approach of [27], which avoids semidefinite programming and is therefore more robust to numerical errors. Finally, we will seek to further generalize our small-gain theorem to enable compositional reasoning with CBFs that are

guaranteed to satisfy the decay requirement over level sets, instead of the entire state and input spaces.

**Acknowledgments:** We would like to thank the anonymous reviewers for their valuable comments. Research supported in part by NSF grants CCF-0926190 and CCF-1018459, and by AFOSR grant FA0550-09-1-0481.

## 9. REFERENCES

- [1] A. Girard. A composition theorem for bisimulation functions. *Pre-print*, 2007. arXiv:1304.5153.
- [2] A. Murthy, M. A. Islam, E. Bartocci, E. Cherry, F. H. Fenton, J. Glimm, S. A. Smolka, and R. Grosu. Approximate bisimulations for sodium channel dynamics. In *Proceedings of CMSB'12, the 10th Conference on Computational Methods in Systems Biology*, LNCS, London, U.K., October 2012. Springer.
- [3] F. L. Bauer and C. T. Fike. *Norms and Exclusion Theorems*. Numerische Mathematik, 1960.

- [4] P. S. Duggirala, S. Mitra, and M. Viswanathan. Verification of annotated models from executions. In *Proceedings of the Eleventh ACM International Conference on Embedded Software, EMSOFT '13*, pages 26:1–26:10, Piscataway, NJ, USA, 2013. IEEE Press.
- [5] S. Gao, J. Avigad, and E. M. Clarke. Delta-complete decision procedures for satisfiability over the reals. In *Proceedings of the 6th International Joint Conference on Automated Reasoning, IJCAR'12*, pages 286–300, Berlin, Heidelberg, 2012. Springer-Verlag.
- [6] S. Gao, J. Avigad, and E. M. Clarke. Delta-decidability over the reals. In *Proceedings of the 27th Annual IEEE Symposium on Logic in Computer Science (LICS), 2012*, pages 305–314. IEEE, 2012.
- [7] S. Gao, S. Kong, and E. M. Clarke. dreal: An SMT solver for nonlinear theories over the reals. In *Automated Deduction—CADE-24*, pages 208–214. Springer, 2013.
- [8] A. Girard and G. J. Pappas. Approximate bisimulations for nonlinear dynamical systems. In *Proceedings of 44th IEEE Conference on Decision and Control*, Seville, Spain, December 2005.
- [9] A. Girard and G. J. Pappas. Approximate bisimulation relations for constrained linear systems. *Automatica*, 43(8):1307 – 1317, August 2007.
- [10] A. Girard and G. J. Pappas. Approximation metrics for discrete and continuous systems. *IEEE Transactions on Automatic Control*, 52(5):782 –798, May 2007.
- [11] A. Girard and G. J. Pappas. Hierarchical control system design using approximate simulation. *Automatica*, 45(2):566 – 571, 2009.
- [12] Z. Huang, C. Fan, A. Mereacre, S. Mitra, and M. Kwiatkowska. Invariant verification of nonlinear hybrid automata networks of cardiac cells. In *Proceedings of 26th International Conference on Computer Aided Verification (CAV)*, volume 8559 of *LNCS*, pages 373–390. Springer, 2014.
- [13] M. A. Islam, A. Murthy, E. Bartocci, E. M. Cherry, F. H. Fenton, J. Glimm, S. A. Smolka, and R. Grosu. Model-order reduction of ion channel dynamics using approximate bisimulation. *Theoretical Computer Science*, 2014.
- [14] H. Jeffreys and B. Jeffreys. *Methods of Mathematical Physics*. Cambridge Mathematical Library, 2000.
- [15] A. A. Julius and G. J. Pappas. Approximate equivalence and approximate synchronization of metric transition systems. In *Proceedings of 45th IEEE Conference on Decision and Control*, San Diego, CA, 2006, December 2006.
- [16] J. Kapinski, J. V. Deshmukh, S. Sankaranarayanan, and N. Arechiga. Simulation-guided Lyapunov analysis for hybrid dynamical systems. In *Hybrid Systems: Computation and Control (HSCC)*, pages 133–142. ACM Press, 2014.
- [17] J. Kapinski, A. Donzé, F. Lerda, H. Maka, S. Wagner, and B. H. Krogh. Control software model checking using bisimulation functions for nonlinear systems. In *47th IEEE Conference on Decision and Control (CDC)*, pages 4024–4029, 2008.
- [18] D. Liberzon. *Switching in Systems and Control*. Springer, 2003.
- [19] J. Lygeros, G. Pappas, and S. Sastry. An introduction to hybrid systems modeling, analysis and control. In *Preprints of the First Nonlinear Control Network Pedagogical School*, pages 307–329, 1999.
- [20] M. A. Islam and A. Murthy. Supplementary document. [www.cs.sunysb.edu/~amurthy/hsc15\\_supp.htm](http://www.cs.sunysb.edu/~amurthy/hsc15_supp.htm), 2014.
- [21] M. A. Islam, A. Murthy, A. Girard, S. A. Smolka, and R. Grosu. Compositionality results for cardiac cell dynamics. In *Proceedings of the 17th International Conference on Hybrid Systems: Computation and Control*. ACM, 2014.
- [22] MATLAB Open curve fitting toolbox (cftool). *Version 7.10.0 (R2010a)*. The MathWorks Inc., Natick, Massachusetts, 2010.
- [23] R. Milner. *Communication and Concurrency*. Prentice Hall, 1989.
- [24] S. Prajna and A. Jadbabaie. Safety verification of hybrid systems using barrier certificates. In *In Hybrid Systems: Computation and Control*, pages 477–492. Springer, 2004.
- [25] S. Prajna, A. Jadbabaie, and G. J. Pappas. A framework for worst-case and stochastic safety verification using barrier certificates. *IEEE Transactions on Automatic Control*, 52(8):1415–1429, 2007.
- [26] S. Prajna, A. Papachristodoulou, P. Seiler, and P. A. Parrilo. *SOSTOOLS: Sum of squares optimization toolbox for MATLAB*, 2004.
- [27] S. Sankaranarayanan, X. Chen, and E. Abraham. Lyapunov function synthesis using Handelman representations. In *IFAC conference on Nonlinear Control Systems (NOLCOS)*, pages 576–581, 2013.
- [28] M. A. B. Sassi, S. Sankaranarayanan, X. Chen, and E. Abraham. Linear relaxations of polynomial positivity for polynomial Lyapunov function synthesis, 2014.
- [29] E. D. Sontag. Smooth stabilization implies coprime factorization. *IEEE Transactions on Automatic Control*, 34(4), 1989.
- [30] E. D. Sontag. On the input-to-state stability property. *Systems and Control Letters*, 24:351–359, 1995.
- [31] E. D. Sontag. Input to state stability: Basic concepts and results. In *Nonlinear and Optimal Control Theory*, pages 163–220. Springer, 2006.
- [32] V. Iyer, R. Mazhari, and R. L. Winslow. A computational model of the human left-ventricular epicardial myocytes. *Biophysical Journal*, 87(3):1507–1525, 2004.
- [33] V. A. Yakubovich, G. A. Leonov, and A. K. Gel'g. Stationary sets in control systems with discontinuous nonlinearities (series on stability, vibration and control of systems, series a, vol. 14), 2004.
- [34] Z. P. Jiang, I. M. Y. Mareels, and Y. Wang. A Lyapunov formulation of the nonlinear small-gain theorem for interconnected ISS systems. *Automatica*, 32(8):1211 – 1215, 1996.